Proceedings of the Institute of Acoustics

SEABED CHARACTERIZATION WITH MULTI-BAND INTERFEROMETRIC SONAR

R van Vossen	TNO, The Hague, The Netherlands
JJM van de Sande	TNO, The Hague, The Netherlands
AJ Duijster	TNO, The Hague, The Netherlands
DW van der Burg	TNO, The Hague, The Netherlands
I Mulders	TNO, The Hague, The Netherlands
ALD Beckers	TNO, The Hague, The Netherlands

INTRODUCTION

Synthetic aperture sonar (SAS) is a key technique for imaging the seabed[1]. It has been shown that low frequency (LF) SAS systems are capable to map the subsurface as well[2]. LF-SAS systems are also able to detect buried objects, such as cables, unexploded ordnance (UXO) or other objects of interest. The usage of LF-SAS systems, however, requires knowledge on the environment in order to determine up to which range and depth objects of interest are detectable. The environment has impact on the signal, i.e. the Target-In-Environment-Response (TIER)[3,4] and on the reverberation. A sound speed contrast between water and seabed sediment results in a critical angle of incidence, and consequently a limited detection range. Attenuation of sound in the seabed limits the depth up to which objects are detectable for a given frequency. There are several mechanisms contributing to reverberation. They include scattering at the seabed, volume scattering at inhomogeneities, including the presence of gas in the sediment, and scattering at sub-seabed interfaces[5]. Because of the impact of the seabed conditions on LF-SAS performance, it is relevant to investigate which information can be retrieved from the data acquired by such a system. This is explored in this paper by developing dedicated data analysis techniques, applied to data acquired in the Haringvliet former estuary (The Netherlands) by TNO's Mine Underground Detection (MUD) system[6].

This paper is organized as follows: Section 2 introduces environmental assessment using a multi-band interferometric synthetic aperture sonar system. Section 3 presents the results of the application of the environmental assessment to data acquired in the Haringvliet, The Netherlands. Conclusions are drawn in Section 4.

MULTI-BAND INTERFEROMETRIC SYNTHETIC APERTURE SONAR

The MUD system (Figure 1) has been developed to detect and localize buried objects in the seabed in inshore environments, such as harbours. It uses LF-SAS as primary sensor to detect buried objects. The sonar system is mounted on an adjustable frame that can be lowered from a moonpool. The system operates in a sidelooking geometry, and the tilt angle of the frame can be adjusted to optimize the performance in different environmental conditions. The system has a 1D projector array and a full 2D receiver array to enable SAS processing in shallow water, and to mitigate distortions in SAS imaging due to multipath in shallow water. The LF-SAS system uses frequencies below 30 kHz.

The LF-SAS is complemented by an interferometric high-frequency SSS to aid the detection and classification of proud objects. The HF-SSS operates at a center frequency on the order of 500 kHz. As will be demonstrated in this paper, the HF interferometric SSS is also required to estimate the depth of burial of objects located in soft seabed sediments.

(a) (b) (c)

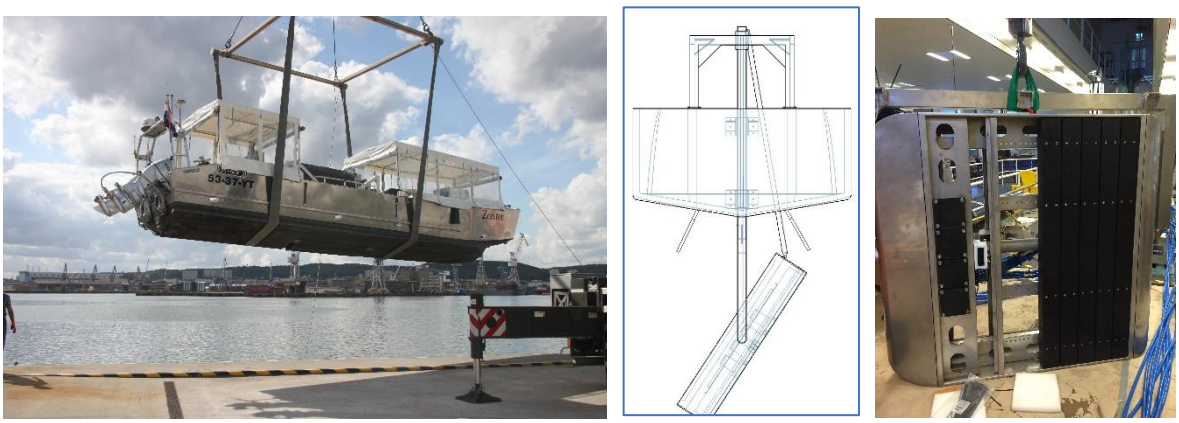

Figure 1: a) Photograph of the MUD system; b) Drawing of MUD system with adjustable sonar frame beneath the platform, and c) Photograph of sonar frame.

Figure 2 presents MUD system imagery for a buried object in multiple frequency bands. It shows that the buried object is clearly detectable in both LF-SAS images, whereas it is not detectable in the corresponding HF-SSS image. Another interesting observation is the large variability in the reverberation between the two LF-SAS images that correspond to different frequency bands.

To gain understanding on the differences observed between the two LF-SAS images, interferometric coherence images[7] for the scene are generated as well (Figure 2d and e), corresponding to both LF-SAS images. In the lower band, a high coherence is observed on the full range, whereas in the upper band, the coherence quickly drops for ranges beyond 10 m. A high interferometric coherence indicates that signals acquired on two vertical sub-arrays have a high correlation. This occurs when dominant scattering occurs at a single depth, for example when interface scattering is dominant. A reduction in the interferometric coherence indicates decorrelation between signals received at two sub-arrays. This suggests that scattering then occurs at multiple depths simultaneously, and could be attributed both to interface and volume scattering.

When a high interferometric coherence is observed, interferometry can be used to estimate the corresponding height of the main scatterer. For this reason, interferometric sonar is suitable to map the bathymetry in high resolution, and also to obtain information on the height of objects located at the seabed[8]. For interferometric LF-SAS, however, interferometry will provide information on the position of the dominant scatterer, which is not necessarily the seabed. In the case study presented in the next section, it is illustrated which information on the seabed can be obtained using a multi-band interferometric sonar system. We only consider the frequency bands in which a high interferometric coherence is obtained. When a low interferometric coherence is obtained, the corresponding height estimate is not reliable.

HARINGVLIET CASE STUDY

Environment

The Haringvliet is situated in the South-Western part of the Netherlands, and is a part of the Rhine-Meuse River delta (Figure 3a). The former estuary is closed off from the sea by the Haringvliet barrier, which has been completed in 1971, as part of the Delta Works to protect the inland from flooding. Since then, it is not influenced by tidal currents, resulting in the deposition of fine sediments. As a result, the seabed consists of a layer of fine silt or mud, with variable thickness, and sand underneath. The sand has complex sedimentation structures corresponding to the regime of a fluvial-tidal transition zone[9,10].

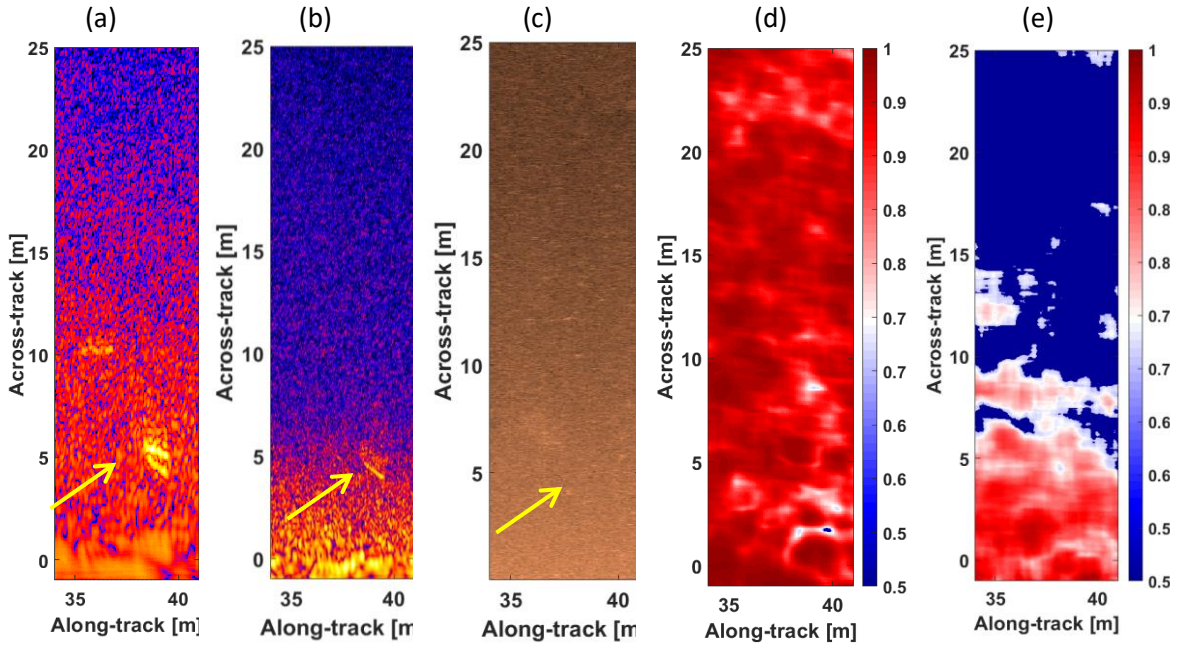

Figure 2: Imagery from different frequency bands, and the corresponding interferometric coherence; a) lower band LF-SAS image; b) upper band LF-SAS image; c) HF-SSS image; d) interferometric coherence corresponding to a);e) interferometric coherence corresponding to b). The arrow indicates the position of a buried object (cylinder).

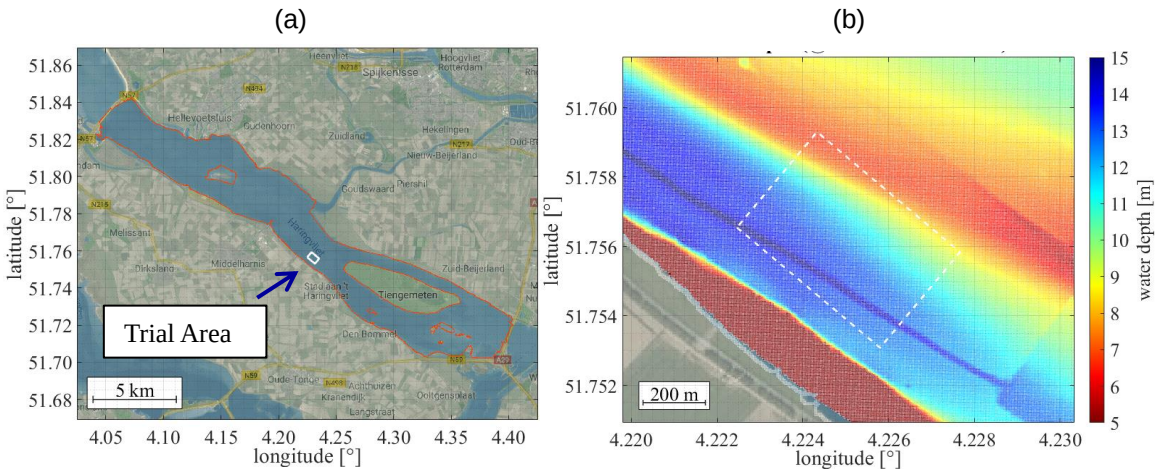

Figure 3: a) Map of Haringvliet and location of trial area (white box); b) Water depth in trial area.

The water depth varies between 0 and 15 m in the Haringvliet, with the exception of a few areas with larger water depths caused by dredging. Dredging activities also occurred in the vicinity of the area considered in the current study, with sediment being removed in the south-eastern part and transported through a channel which intersects with the trial area as part of soil remediation projects (Figure 3b).

Multi-band synthetic aperture sonar imagery

Figure 4 presents georeferenced multi-band sonar imagery from the Haringvliet environment. The HF-SSS image shown in Figure 4a hardly reveals differences in intensity, except at the position of a proud object. This is expected for a flat interface between water and a mud or silt layer. The corresponding LF-SAS image, on the other hand, reveals significant differences in the scattering intensity (> 10 dB). Because of this variability, it is also harder to identify the scattering that originates from the proud object. The hypothesis is that the scattering observed in the LF-SAS image is either caused by volume scattering within the sediment or by interface scattering at subsurface layers, and not by scattering at the water/mud interface. This hypothesis will be further analysed by considering multi-band interferometric height estimates.

Multi-band interferometric height estimates

Multi-band interferometric height estimates corresponding to Figure 4 are presented in Figure 5. It can be observed that the height estimates derived from HF-SSS differ from the LF-SAS height estimates, except for a proud object. This is a concrete block. The height differences are on the order of 0.7-0.9 m. For the proud object, the HF-SSS and LF-SAS interferometric height estimates are within 0.05 m.

The explanation for the differences between the HF-SSS and LF-SAS interferometric height estimates are the scattering mechanisms. For HF-SSS, dominant scattering occurs at the water/mud interface. Due to high absorption of high-frequency sound in seabed sediments, it has very limited penetration into the seabed. For LF-SAS, on the other hand, the attenuation is limited, and the mud layer becomes acoustically transparent. This means that the LF-SAS scattering intensity images (Figure 4) do not reveal the presence of the mud layer. The interferometric coherence (Figure 2) indicates that dominant scattering occurs at a single height, ruling out volume scattering. This leads to the interpretation that dominant scattering occurs at the mud/sand interface in this frequency band. The variability observed in both the height estimates and in the scattering intensity is indicative for the presence of wave ripples or complexity in the scattering response within the sand layer, originating from the time that the Haringvliet still was an estuary[9,10,] .

The results presented in Figure 2-Figure 5 show that the multi-band interferometric sonar system is capable of mapping a volume of sediment in the Haringvliet environment, where a soft sediment layer is encountered with sand underneath. Furthermore, it is demonstrated that buried objects can be detected in the sediment volume, including the 3D localization. The localization does not only include the position (x,y), but also the burial depth (z). In the next section, the sediment characterization results are compared to measurements derived from a downlooking sub-bottom profiler geometry.

Comparison with sub-bottom profiler geometry

The results presented in the previous sections use the MUD system in sidelooking mode. This mode results in an increased area coverage rate compared to a downlooking mode. The downlooking mode, on the other hand, is a more common geometry for acquiring information on layering of the seabed. In the downlooking mode, the MUD system essentially becomes a sub-bottom profiler (SBP). With a SBP, information on layering of the seabed can be directly derived from the data. A SBP, however, is not directly suitable to map an area, especially when discrete objects are to be detected, because a SBP maps the seabed in cross-sections.

Figure 6 shows a downlooking image obtained with the MUD system. It indeed reveals the presence of a soft sediment layer. A weak reflection is observed at the water/mud interface, whereas the reflection at the mud/sand interface is stronger. The thickness of the mud layer is in agreement with the thickness derived from the multi-band interferometric height estimates.

The high backscattering intensity in the depth window between 11 and 12 m suggests that there is significant scattering within the sand layer, whereas there is hardly any volume scattering in the mud layer. This result is expected based on the complex morphology of fluvial-tidal sediments[9,10].

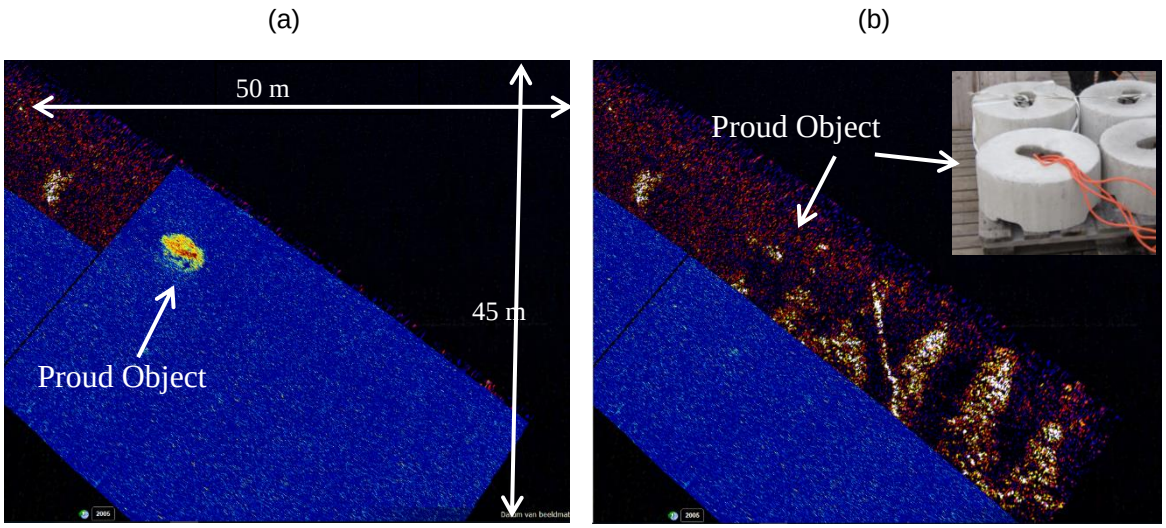

Figure 4: a) Georeferenced images obtained with the HF-SSS (top layer with blue-yellow-red color scale with high intensity in red) and b) with the LF-SAS (black-red-yellow, with high intensity in yellow (decibel scale). A contact corresponding to a proud object (concrete block, see photo) is indicated by an arrow in both images.

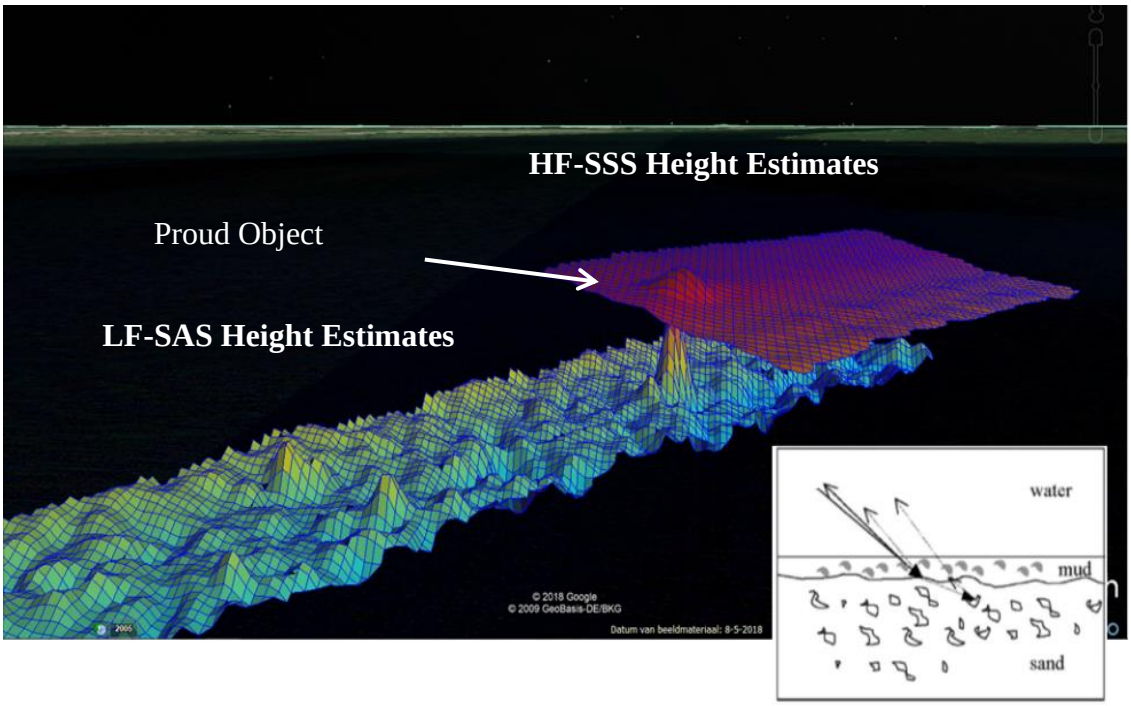

Figure 5: 3D view of interferometric height estimates obtained from LF-SAS and HF-SSS. The arrow indicates the proud object. The inset is a schematic illustration of the scenario[5].

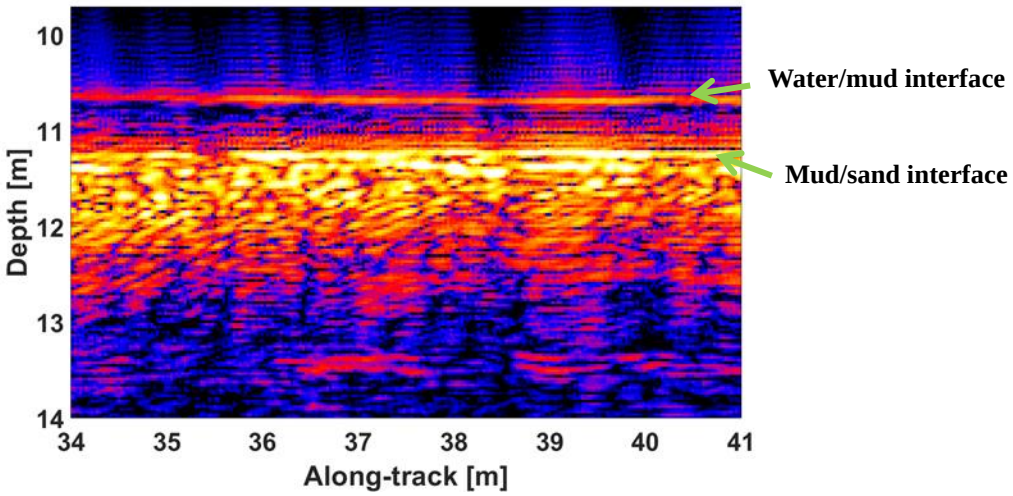

Figure 6: Downlooking image of the MUD system.

Comparison to mud layer thickness measurements

In the Haringvliet, dedicated studies have been conducted to measure and monitor the mud layer thickness, including erosion and sedimentation to support soil remediation[11]. These studies investigated the feasibility of using different dredging techniques for the removal of contaminated soil, and require detailed mapping of the mud layer in the Haringvliet as input. In the RWS studies (Rijkswaterstaat), the mud layer thickness is determined combining SBP measurements with a large number of in-situ soil auger measurements.

Figure 7 compares the mud layer thickness derived from the multi-band interferometric sonar measurements conducted in 2019 to the thickness reported in the 2009 RWS study. Despite the 10 year time difference, there is an overall good agreement between the RWS and MUD system measurements. The main differences are observed in the vicinity of the channel in the southwestern part of the area, which has been used to transport contaminated sediment with fluid-injection dredging. Due to the variability in the bathymetry close to the channel (Figure 3), erosion is to be expected at the edges of the channel. This result is indeed obtained when the RWS results are compared to the MUD results. The second observation is that the mud-layer thickness estimated using the MUD system is generally higher than the thickness reported in the RWS study. This result is also not surprising, because of the 10-years time difference and the continuing sedimentation.

CONCLUSIONS

This paper introduces multi-band interferometric sonar as a technique to map a sediment volume in an efficient fashion. Potential use cases for this type of environmental assessment are soil remediation, i.e. to map the extent of contaminated fluvial seabed sediments, and the detection of buried objects, such as cables, pipelines and unexploded ordnance (UXO). The Haringvliet case study results demonstrate that (i) buried objects can be detected and localized, including the depth of burial, and (ii) that the thickness of soft sediment layers can be accurately mapped using the wideband interferometric sonar system.

ACKNOWLEDGEMENTS

The authors acknowledge the Netherlands Ministry of Defence and the United States Department of Defense Strategic Environmental Research and Development Program (SERDP) for sponsoring. Rijkswaterstaat is acknowledged for providing the reference data.

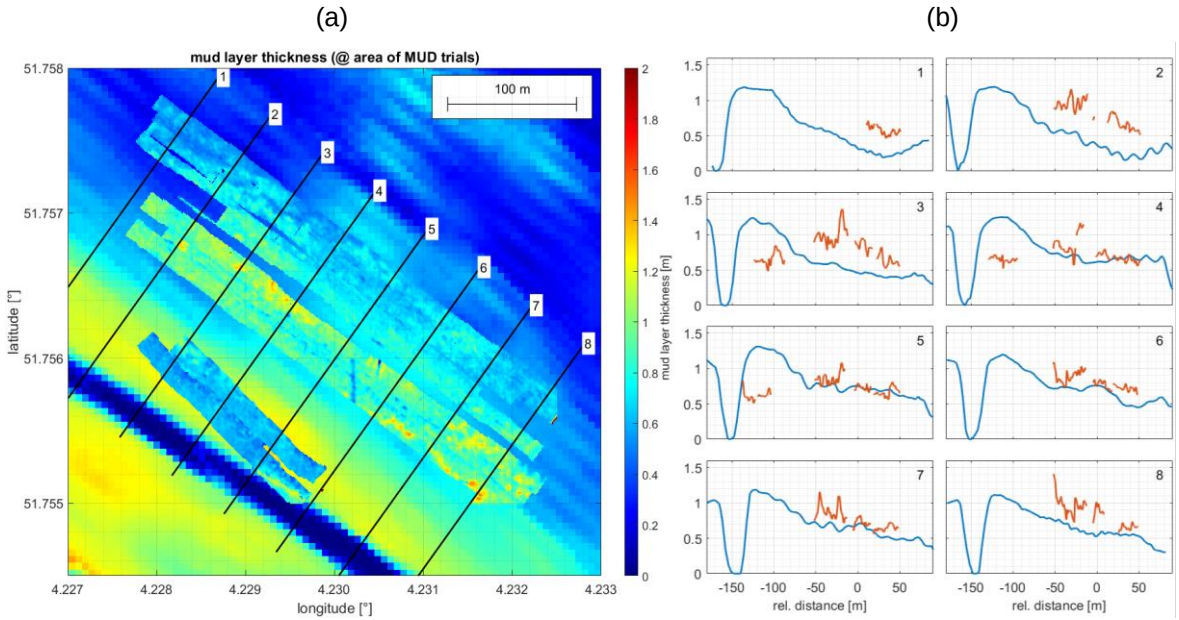

Figure 7: a) Map with mud layer thickness from RWS study, with the high-resolution mud layer thickness obtained from the multi-band interferometric MUD system plotted on top; b) mud layer thickness along lines 1-8 in figure a), with RWS results in blue and high-resolution MUD system results in red.

REFERENCES

1. R. E. Hansen, “Introduction to synthetic aperture sonar”, in *Sonar Systems*, InTechOpen, 3-28 (2011).
2. D. D. Sternlicht, J. E. Fernandez, R. Holtzapple, D. P. Kucik, T. C. Montgomery and C. M. Loeffler, “Advanced sonar technologies for autonomous mine countermeasures”, in *MTS/IEEE Oceans*, Waikoloa HI, USA, (2011).
3. K. L. Williams, S. G. Kargl, E. I. Thorsos, D. S. Burnett, J. L. Lopes, M. Zampolli and P. L. Marston, “Acoustic scattering from a solid aluminum cylinder in contact with a sand sediment: Measurements, modeling, and interpretation”, *J. Acoust. Soc. Am.,* **127**, 3356-3371 (2010).
4. S. G. Kargl, A. L. España, K. L. Williams, J. L. Kennedy and J. L. Lopes, “Scattering from objects at a water-sediment interface: Experiment, high-speed, and high-fidelity models, and physical insight,” *IEEE Journal of Oceanic Engineering*”, **40**, 632-642, (2015).
5. K. L. Williams, D. R. Jackson, D. B. K. B. Tang and E. I. Thorsos, “Acoustic backscattering from a sand and a sand/mud environment: Experiments and data/model comparisons”, *IEEE Journal of Oceanic Engineering*, **34**, 388-398, (2009).
6. A. L. D. Beckers, “The hunt for buried objects”, in Maritime Air Systems & Technologies (MAST), Amsterdam, (2016).
7. S. A. Synnes, R. E. Hansen and T. O. Saebo, “Assessment of shallow water performance using interferometric sonar coherence”, in *Underwater Acoustic Measurements (UAM)*, Nafplion, Greece, (2009).
8. T. O. Saebo, H. J. Callow, R. E. Hansen, B. Langli and E. O. Hammerstad, “Bathymetric capabilities of the HISAS interferometric synthetic aperture sonar”, in *OCEANS*, Vancouver BC, Canada, (2007).
9. E. Oomkens and J. H. J. Terwindt, “Inshore estuarine sediments in the Haringvliet (Netherlands)”, *Netherlands Journal of Geosciences - Geologie en Mijnbouw*, **39**, 701-710, (1960).

10. J. H. van den Berg, J. R. Boersma and A. van Gelder, „Diagnostic sedimentary structures of the fluvial-tidal transition zone - Evidence from deposits of the Rhine and Meuse," *Netherlands Journal of Geosciences - Geologie en Mijnbouw*, **86**, 287-306, (2007).

11. "Meetrapport waterbodemonderzoek Haringvliet-Oost", Rijkswaterstaat Zuid-Holland, (2009).